Kaempferol induces apoptosis in glioblastoma cells through oxidative stress

Vivek Sharma, Christy Joseph, Soumya Ghosh, Anindita Agarwal, Manoj Kumar Mishra, and Ellora Sen

National Brain Research Centre, Manesar, Haryana, India

Abstract

Despite recent advances in understanding molecular mechanisms involved in glioblastoma progression, the prognosis of the most malignant brain tumor continues to be dismal. Because the flavonoid kaempferol is known to suppress growth of a number of human malignancies, we investigated the effect of kaempferol on human glioblastoma cells. Kaempferol induced apoptosis in glioma cells by elevating intracellular oxidative stress. Heightened oxidative stress was characterized by an increased generation of reactive oxygen species (ROS) accompanied by a decrease in oxidant-scavenging agents such as superoxide dismutase (SOD-1) and thioredoxin (TRX-1). Knockdown of SOD-1 and TRX-1 expression by small interfering RNA (siRNA) increased ROS generation and sensitivity of glioma cells to kaempferol-induced apoptosis. Signs of apoptosis included decreased expression of Bcl-2 and altered mitochondrial membrane potential with elevated active caspase-3 and cleaved poly(ADP-ribose) polymerase expression. Plasma membrane potential and membrane fluidity were altered in kaempferol-treated cells. Kaempferol suppressed the expression of proinflammatory cytokine interleukin-6 and chemokines interleukin-8, monocyte chemoattractant protein-1, and regulated on activation, normal T-cell expressed and secreted. Kaempferol inhibited glioma cell migration in a ROS-dependent manner. Importantly, kaempferol potentiated the toxic effect of chemotherapeutic agent doxorubicin by amplifying ROS toxicity and decreasing the efflux of doxorubicin. Because the toxic effect of both kaempferol and doxorubicin was amplified when used in combination, this study raises the possibility of combinatorial therapy whose basis constitutes enhancing redox perturbation as a strategy to kill glioma cells. [Mol Cancer Ther 2007;6(9):2544–53]

Received 12/21/06; revised 7/3/07; accepted 8/2/07.

Grant support: Department of Biotechnology, Government of India, to the National Brain Research Centre, Manesar, and partly by a research grant from Department of Biotechnology (E. Sen).

The costs of publication of this article were defrayed in part by the payment of page charges. This article must therefore be hereby marked *advertisement* in accordance with 18 U.S.C. Section 1734 solely to indicate this fact.

Requests for reprints: Ellora Sen, National Brain Research Centre, near NSG Campus, Manesar, Gurgaon, Haryana-122050, India. Phone: 91-12-4233-8921, ext. 235; Fax: 91-12-4233-8910/28. E-mail: ellora@nbrc.res.in

doi:10.1158/1535-7163.MCT-06-0788

Introduction

Reactive oxygen species (ROS) are released by the normal oxidative metabolism in eukaryotic cells, and cellular antioxidants such as superoxide dismutase (SOD-1) and thioredoxin (TRX-1) detoxify these species. However, ROS overproduction or a decrease in the antioxidative capacity of cells can cause oxidative stress (1). Most cancer cells are under oxidative stress associated with increased metabolic activity and production of ROS (2). Although increased ROS production plays an important role in maintaining cancer phenotype due to their stimulating effects on cell growth and proliferation (3), high levels of ROS can also cause cellular damage (4). ROS-stressing agents can effectively kill cancer cells by increasing the intracellular ROS to a toxic level (5). Human cancer cells with intrinsic oxidative stress are highly sensitive to ROS stress (6, 7) and promoting ROS generation in mitochondria can effectively kill them (4).

The anticancer activity of flavonoids, a group of polyphenolic compounds, has been well shown (8). Flavonoids exhibit anticancer activity by elevating ROS generation (9) and by inhibiting thioredoxin reductase, which is critical for maintaining the cellular redox environment (10). The flavonoid kaempferol is known to possess cancer chemopreventive properties (11, 12) and to inhibit migration and invasiveness of glioma cells (13). A heightened oxidative stress seems to be characteristic of gliomas, with elevation in ROS production increasing the resistance of cells to chemotherapy (14, 15). Because kaempferol alters ROS generation (16, 17), we investigated whether kaempferol could be used as a redox-modulating agent to induce apoptosis in glioma cells by increasing ROS accumulation while concomitantly disabling the antioxidant defense mechanism. Because the anticancer drug doxorubicin exerts its cytotoxic effect on tumor cells through generation of ROS (18), we also investigated whether kaempferol could potentiate the toxic effects of doxorubicin by elevating oxidative stress.

Materials and Methods

Cell Culture and Treatment

Glioblastoma cell lines LN229, U87MG, and T98G were obtained from the American Type Culture Collection. Cells were cultured in DMEM (Life Technologies, Inc.) supplemented with 10% fetal bovine serum, 100 units/L penicillin, and 100 μg/mL streptomycin (Life Technologies). On attaining semiconfluence, medium was depleted of fetal bovine serum and all treatments were carried out in serum-free medium. The cells were treated with

50 μmol/L kaempferol (in DMSO) for different intervals of time (24, 48, 72, and 96 h). DMSO-treated cells were used as controls. To study whether kaempferol alters the sensitivity of cells to doxorubicin, the cells were treated with 1 μmol/L doxorubicin in the presence and absence of kaempferol for 24 h. To determine the involvement of ROS in cell death, ROS-specific inhibitor *N*-acetylcysteine (NAC) was added to cells either alone or in combination with kaempferol. For all treatments involving NAC, 1 mmol/L NAC was administered simultaneously with kaempferol. All reagents were purchased from Sigma unless otherwise stated.

Determination of Cell Viability

Cell viability was assessed using the [3-(4,5-dimethylthiazol-2-yl)-5-(3-carboxymethoxyphenyl)-2-(4-sulfophenyl)-2*H*-tetrazolium, inner salt] (MTS; Promega) assay as described earlier (19). Following treatment of cells (1×10^3) with kaempferol for different time intervals in 96-well plates, 20 μL of MTS solution were added. After 4-h incubation, the absorbance reflecting reduction of MTS by viable cells was determined at 490 nm. Values were expressed as a percentage relative to those obtained in controls.

Terminal Deoxyribonucleotidyl Transferase–Mediated dUTP Nick End Labeling Assay

Glioma cells (10^4) were treated with kaempferol, doxorubicin, or NAC, either alone or in different combinations for different time intervals, in eight-well chamber slides (Nunc). Following treatment, apoptotic cells were identified using In Situ Cell Death Detection Kit, TMR red (Roche). Briefly, cells were fixed with 4% paraformaldehyde in PBS and blocked with 4% bovine serum albumin containing 0.02% Triton X-100, and then fixed cells were incubated in the terminal deoxyribonucleotidyl transferase–mediated dUTP nick end labeling (TUNEL) mix (terminal deoxynucleotidyl transferase in storage buffer and TMR red–labeled nucleotide mixture in reaction buffer) for 1 h at room temperature. The slides were mounted with Vectashield mounting medium containing 4′,6-diamidino-2-phenylindole (Vector Laboratories, Inc.). Cell death was determined by counting the number of TUNEL-positive cells (red) that colocalized with 4′,6-diamidino-2-phenylindole (blue) from multiple fields.

Measurement of ROS

Intracellular ROS generation in cells treated with kaempferol or doxorubicin, or a combination of both, and in kaempferol-treated cells transfected with SOD-1 or TRX-1, or both small interfering RNA (siRNA), was assessed using 2′,7′-dichlorodihydrofluorescein diacetate (CM-H_2DCFDA; Molecular Probes) as previously described (20) with some modifications. Briefly, cells were incubated with H_2DCFDA (5 μmol/L) for 30 min at 37°C and washed twice with PBS, and then fluorescence intensity of 5×10^5 cells was measured with a spectrofluorometer (excitation, 500 nm; emission, 530 nm).

siRNA Transfection

LN229 and U87MG cells were transfected with SOD-1 and TRX-1 siRNA as previously described (21). Briefly, 18 h before transfection, 2×10^4 cells were seeded onto 24-well plates in medium without antibiotics and transfection of siRNAs was carried out with Lipofectamine 2000 (Life Technologies-Invitrogen) as per manufacturer's instruction. All transfections were carried out with 50 nmol/L duplex siRNA. After 48 h, the viability of transfected cells was determined by MTS assay. In addition, cells were harvested 48 h following transfection and Western blot analysis was done to determine the level of SOD-1 and TRX-1 in transfected cells. Transfected cells were then either left untreated or treated with 50 μmol/L kaempferol for additional 48 h in fresh medium and cell viability was determined by MTS assay. The siRNA duplexes were synthesized by Proligo. Transfection with nonspecific siRNA against Luciferase GL2 was done as control. The sequences of siRNA used were as follows: siTRX, 5′-AUGACUGUCAGGAUGUUGCdTdT-3′ (sense) and 5′-GCAACAUCCUGACAGUCAUdCdC-3′ (antisense); siSOD-1, 5′-GGCCUGCAUGGAUUCCAUGdTdT-3′ (sense) and 5′CAUGGAAUCCAUGCAGGCCdTdT-3′ (antisense).

Immunoblotting

Protein was isolated from control and kaempferol-treated cells as previously described (22). Twenty micrograms of each sample were electrophoresed on a 6% to 10% polyacrylamide gel and Western blot analysis was done, as previously described (22), with SOD-1 and TRX-1 antibodies (Lab Frontier). Antibodies were purchased from Santa Cruz Biotechnology unless otherwise mentioned. Secondary antibodies were purchased from Vector Laboratories. After addition of chemiluminescence reagent (Amersham), the blots were exposed to ChemiGenius Bioimaging System (Syngene) for developing and images were captured using Genesnap software (Syngene). Absorbance measurements were made using Gentools software (Syngene). The blots were stripped and reprobed with anti–β-tubulin to determine equivalent loading as described (23).

Determination of Mitochondrial Membrane Potential

Mitochondrial membrane potential ($\Delta\Psi_m$) was measured using JC-1 probe (20). To measure $\Delta\Psi_m$, control and kaempferol-treated cells were labeled for 40 min with 6.5 μmol/L JC-1 at 37°C, washed, and resuspended in medium; fluorescence was recorded at 590 and 527 nm. The ratio of the reading at 590 to 527 nm was considered as the relative $\Delta\Psi_m$ value. JC-1 accumulates as J-aggregates (590 nm; red) only in metabolically active mitochondria and depolarization of mitochondrial membranes leads to JC-1 monomer formation (527 nm; green). Control and kaempferol-treated cells were also labeled for 10 min with 10 μmol/L JC-1 at 37°C and cells were examined by fluorescence microscopy (20).

Measurement of Plasma Membrane Potential

Membrane potential of control and kaempferol-treated cells was assessed by flow cytometry using negatively charged $DiBAC_4(3)$ oxonol dye (Molecular Probes; ref. 24). Briefly, 10^6 cells/mL were equilibrated for 1 min in PBS followed by the addition of 150 nmol/L oxonol. After equilibration for 2 min, oxonol fluorescence intensity of 5×10^4 cells was measured by FACSCalibur (Becton

Dickinson) with acquisition of fluorescence emission at the FL1 spectrum versus SSC, as previously described (25). As a positive control for membrane depolarization, cells were incubated with 150 mmol/L KCl for 2 min at 4°C before addition of oxonol dye (24).

Measurement of Membrane Fluorescence Anisotropy

Membrane fluidity of glioma cells treated with kaempferol for 96 h was determined using the fluorescent probe 1,6-diphenyl-1,3,5-hexatriene (DPH) as described (26). Briefly, 2×10^5 control and kaempferol-treated cells were incubated with 1 μmol/L DPH in PBS for 2 h at 37°C, following which cells were washed and resuspended in PBS, and the DPH probe bound to the cell membrane was excited at 365 nm and the emission was recorded at 430 nm by Spectrofluorometer (Varian). The fluorescence anisotropy (r) value was calculated using the equation $r = [(I_{||} - I_{\perp}) / (I_{||} + 2I_{\perp})]$, where $I_{||}$ and $I_{\perp}$ are the fluorescence intensities oriented parallel and perpendicular, respectively, to the direction of polarization of the excited light. The microviscosity parameter $[(r_o / r) - 1]^{-1}$ was calculated in each case knowing the maximal limiting fluorescence anisotropy r_o, which is 0.362 for DPH.

Cytokine and Apoptosis Bead Array

Cytometric bead array kit (CBA kit, BD Biosciences) was used to quantitatively measure cytokine and chemokine levels in the supernatant collected from control and cells treated with kaempferol in the presence or absence of NAC. Human apoptosis kit (BD Biosciences) was used to quantitatively measure the expression levels of active caspase-3, cleaved poly(ADP-ribose) polymerase (PARP), and Bcl-2 in protein lysates collected from control and kaempferol-treated cells. Using 50 μL of human inflammation or apoptosis standard and sample dilutions, the assay was done and analyzed on FACSCalibur (Becton Dickinson) as described (27).

Wound Healing Assay

Cells were grown in medium containing fetal bovine serum and, on reaching semiconfluence, fetal bovine serum was removed and cells were grown in serum-free medium. A plastic pipette tip was drawn across the center of the culture to produce a clean wound area 12 h after serum depletion. Cells were then left untreated or treated with kaempferol in the presence and absence of NAC for 48 and 72 h and cell movement in the wound area was examined. The migration distance between the leading edge of the migrating cells and the edge of the wound at the beginning and end of each indicated time point was taken by light microscopy.

Doxorubicin Accumulation

In studies where doxorubicin accumulation was examined, control and kaempferol-treated U87MG cells (1×10^6) were incubated with 1 μmol/L doxorubicin for 30 min at 37°C and 5% CO_2. Cells were subsequently harvested and washed, and intracellular doxorubicin accumulation was measured by flow cytometry at the FL2 emission spectrum (on FACSCalibur) immediately at $t = 0$ min for accumulation and at $t = 120$ min on further incubation at 37°C and 5% CO_2 to allow for efflux as described (25).

Statistical Analysis

All comparisons between groups were done using two-tailed paired Student's t test. $P < 0.05$ was considered to be significant.

Results

Kaempferol Induces Apoptosis in Human Glioma Cells

To determine whether kaempferol affects viability of glioma cells, MTS assay was done on LN229, U87MG, and T98G cells treated with kaempferol for 24, 48, 72, and 96 h. A time-dependent decrease in cell viability was observed in LN229 cells treated with kaempferol, with significant 36% and 45% reductions in viability occurring at 72 and 96 h, respectively, as compared with control (Fig. 1*A*). A similar trend in loss of viability was observed in U87MG and T98G on kaempferol treatment (Fig. 1*A*).

Because maximal cell death was observed at 96 h post-treatment with kaempferol, we carried out fluorescence-activated cell sorting (FACS) analysis to detect the levels of active caspase-3, cleaved PARP, and Bcl-2 in these cells. Expression of proapoptotic molecules active caspase-3 and cleaved PARP was elevated by 2.3- and 140-fold in

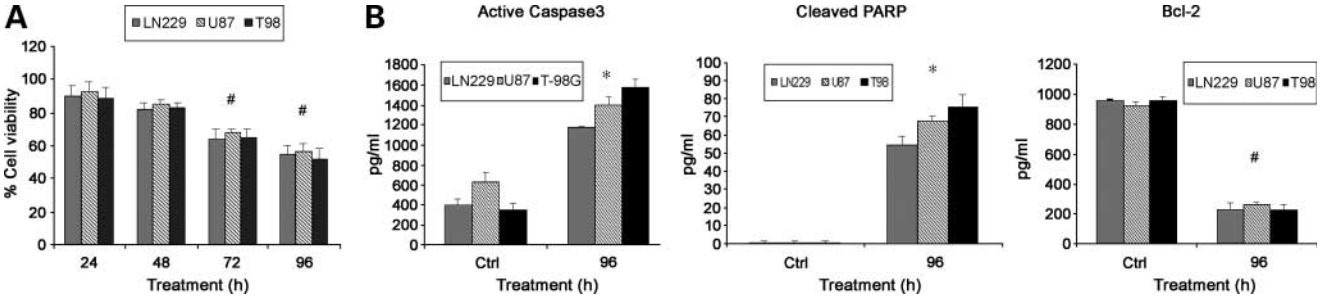

Figure 1. Kaempferol induces apoptosis of glioblastoma cells in a time-dependent manner. **A,** viability of kaempferol-treated glioma cells was determined by MTS assay. The graph represents the percentage viable cells of control observed when U87MG, T98G, and LN229 cells were treated with kaempferol for 24, 48, 72, and 96 h. **B,** levels of active caspase-3, cleaved PARP, and Bcl-2 in U87MG, T98G, and LN229 cells treated with kaempferol for 96 h, as observed by apoptosis bead array. **A** and **B,** *columns,* mean from three independent experiments; *bars,* SE. * and #, $P < 0.05$, significant increase and decrease, respectively, compared with control.

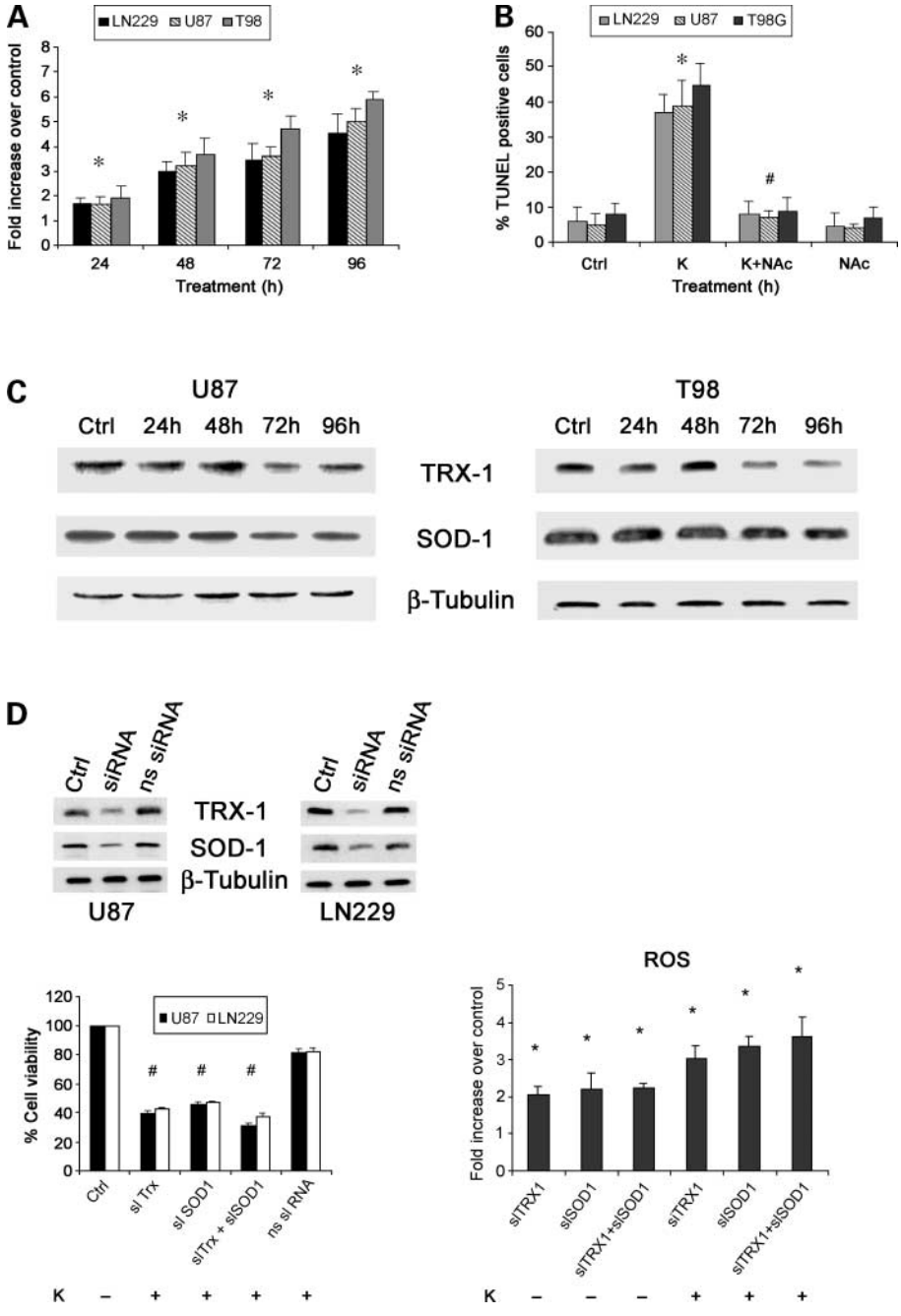

Figure 2. Kaempferol affects the expression of molecules associated with oxidative stress. **A,** ROS generation in U87MG, T98G, and LN229 glioblastoma cells treated with kaempferol for 24, 48, 72, and 96 h. *Columns,* mean fold change in ROS levels over control from three individual experiments; *bars,* SE. *, $P < 0.05$, significant increase compared with control. **B,** ROS inhibitor NAC abolishes kaempferol-induced cytotoxicity because a decrease in TUNEL-positive cells was observed when kaempferol treatment was supplemented with NAC. The graph represents the percentage of TUNEL-positive cells observed when U87MG, T98G, and LN229 cells were treated with either kaempferol or NAC, or a combination of both, for 96 h, as counted from multiple fields. *Columns,* mean from three independent experiments; *bars,* SE. *, $P < 0.05$, significant increase versus control. #, $P < 0.05$, significant decrease versus kaempferol-treated cells. **C,** SOD-1 and TRX-1 expression in gliomas treated with kaempferol for 24, 48, 72, and 96 h, as analyzed by Western blot. A representative blot is shown from three independent experiments with identical results. Blots were reprobed for β-tubulin to establish equivalent loading. **D,** glioma cells transfected with siRNA SOD-1, TRX-1, or both for 48 h were treated with kaempferol for additional 48 h and cell viability was analyzed by MTS assay. A significant decrease in viability was observed in kaempferol-treated cells with down-regulated SOD-1, TRX-1, or both, but not in cells transfected with nonspecific siRNA. Viability of cells transfected with SOD-1 or TRX-1 siRNA alone was taken as control (set at 100%). siRNA-mediated knockdown of SOD-1 and TRX-1 expression in U87MG and LN229 resulted in decreased SOD-1 and TRX-1 levels as determined by Western blot analysis. ROS levels in U87MG, transfected with SOD-1, TRX-1, or both siRNA, in the presence and absence of kaempferol. *Columns,* mean from three independent experiments; *bars,* SE. * and #, $P < 0.05$, significant increase and decrease, respectively, compared with control. *K,* kaempferol; *NS,* nonspecific.

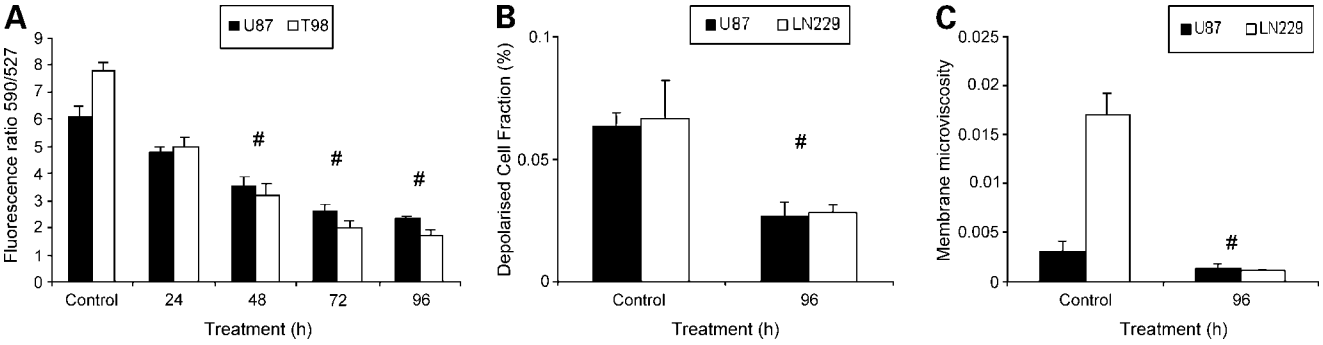

Figure 3. Treatment with kaempferol alters the biophysical parameters of glioma cell membranes. **A,** kaempferol treatment decreases mitochondrial membrane potential. Mitochondrial membrane potential $\Delta\Psi_m$ of control and kaempferol-treated cells as measured by the 590:527 ratio of JC-1 fluorescence intensity. Fluorescence micrographs of kaempferol-treated and untreated U87MG cells stained with JC-1 to show decrease in mitochondrial membrane potential with increased exposure to kaempferol. Micrographs show that JC-1 accumulates within active mitochondria and exhibits orange fluorescence (Supplementary data). **B,** relative membrane potential $\Delta\Psi_p$ of gliomas treated with kaempferol for 96 h as calculated by the fluorescence intensity of oxonol-stained cells acquired at the FL1 emission spectrum versus SSC. The percentage of depolarized cell fraction is shown. **C,** membrane microviscosity of gliomas treated with kaempferol for 96 h as compared with control. Fluorescence intensity of cells labeled with DPH was measured and membrane microviscosity was determined. **A** to **C,** *columns,* mean from three individual experiments; *bars,* SE. #, $P < 0.05$, significant decrease compared with control.

kaempferol-treated U87MG as compared with control (Fig. 1*B*). This was accompanied by a 3.5-fold decrease in the expression of antiapoptotic protein Bcl-2 (Fig. 1*B*). A similar trend in the expression of active caspase-3, cleaved PARP, and Bcl-2 was observed in LN229 and T98G on kaempferol treatment (Fig. 1*B*).

ROS-Mediated Damage Is Critical for Kaempferol-Induced Cell Death

Because ROS have been suggested as a possible mediator of apoptosis induced by kaempferol, we examined ROS production in kaempferol-treated cells using the fluorescent probe DCFDA. A gradual increase in ROS production as compared with control was observed with increasing exposure to kaempferol in U87MG, T98G, and LN229 cells. A significant 3-, 3.5-, and 4.5-fold increase in ROS production was observed in U87MG treated with kaempferol for 48, 72, and 96 h, respectively, as compared with control (Fig. 2*A*). A similar trend in ROS generation was also observed in T98G and LN229 (Fig. 2*A*), with ROS production reaching maximum at 96 h.

To determine whether increased production of ROS following kaempferol treatment was critical in inducing apoptosis, TUNEL staining was done on cells treated with ROS inhibitor NAC in the presence of kaempferol for 96 h. No significant difference in the percentage of apoptotic cell was observed between NAC-treated cells and control (Fig. 2*B*). However, the ~5-fold increase in apoptotic cells observed in all three cell lines treated with kaempferol was significantly reduced to that of control values when kaempferol treatment was supplemented with NAC (Fig. 2*B*). The cytotoxicity of kaempferol was abolished in the presence of ROS inhibitor.

We next determined the status of SOD-1 and TRX-1, which are involved in maintaining cellular redox balance, in kaempferol-treated gliomas with elevated ROS levels. Western blot analysis revealed a decrease in SOD-1 and TRX-1 expression in gliomas with increasing exposure to kaempferol (Fig. 2*C*). While the expression of SOD-1 and TRX-1 in U87MG and T98G treated with kaempferol for 24 and 48 h were comparable to control, a decrease in expression was observed at 72 and 96 h (Fig. 2*C*). Densitometric analysis revealed an ~2.7- and 2.0-fold decrease in TRX-1 and SOD-1 expression, respectively, in cells treated with kaempferol for 96 h as compared with control. A similar trend was observed in LN229 cells (data not shown).

SOD-1 and TRX-1 Knockdown Augments Kaempferol-Induced Apoptosis

Because down-regulation of SOD-1 (28) and TRX-1 (29) expression increases sensitivity of tumor cells to cytotoxic agents, we investigated whether knocking down SOD-1 and TRX-1 expression using siRNA would increase sensitivity of glioma cells to kaempferol-induced apoptosis. The expression of SOD-1 and TRX-1 was down-regulated by >70% in cells transfected with SOD-1 and TRX-1 siRNA at 48 h, as determined by Western blot analysis (Fig. 2*D*). The nonspecific siRNA had no effect on SOD-1 and TRX-1 levels. After 48 h of culture, cells transfected with nonspecific siRNA, SOD-1, TRX-1, or both SOD-1 and TRX-1 siRNA were treated with or without kaempferol for an additional 48 h. SOD-1 and TRX-1 siRNA–transfected cells had decreased cell viability as compared with nontransfected cells or cells transfected with nonspecific siRNA. Kaempferol treatment decreased the viability of SOD-1 and TRX-1 siRNA–transfected cells, on average, by 60% and 55%, respectively, as compared with untreated SOD-1– and TRX-1–transfected control cells (viability set at 100%; Fig. 2*D*). Viability was further decreased in kaempferol-treated cells transfected with a combination of both SOD-1 and TRX-1 siRNA. The decrease in viability in kaempferol-treated cells transfected with nonspecific siRNA was not significant.

In addition, SOD-1 and TRX-1 siRNA–transfected cells had higher average (~2-fold) levels of ROS compared with untransfected control. Importantly, kaempferol treatment

increased the levels of ROS further (~3-fold) in SOD-1 and TRX-1 siRNA–transfected cells (Fig. 2*D*). Thus, SOD-1 and TRX-1 down-regulation augmented kaempferol-induced cytotoxicity in glioma cells by elevating ROS levels.

Kaempferol Decreases Mitochondrial Membrane Potential ($\Delta\Psi_m$) in Glioma Cells

Because ROS generation is inversely correlated with $\Delta\Psi_m$ (30), we investigated mitochondrial changes in terms of alterations in $\Delta\Psi_m$, which is indicative of the status of mitochondrial function. Measurement of JC-1 aggregate (indicative of intact mitochondria) and J-monomer (indicative of de-energized mitochondria) formation (expressed as the ratio of 590:527 fluorescence) showed a gradual but significant decrease in $\Delta\Psi_m$ with progressive treatment of U87MG and T98G cells with kaempferol as compared with control (Fig. 3*A*). Intact mitochondrial function, as indicated by the accumulation of JC-1 orange fluorescence, was observed in control and kaempferol-treated U87MG cells at 24 h (Supplementary data).[1] The absence of detectable JC-1 orange fluorescence in cells treated with kaempferol for 72 and 96 h indicated a diminished $\Delta\Psi_m$ (Supplementary data).[1]

Kaempferol Alters Plasma Membrane Potential $\Delta\psi_p$ of Glioma Cells

Because increased ROS generation causes prolonged membrane hyperpolarization (31) and because kaempferol causes ROS associated alterations of plasma membrane (32), the effect of kaempferol on $\Delta\psi_p$ of glioma cells was investigated. FACS analysis using membrane potential–sensing fluorescent dye oxonol indicated a significant (~2-fold) decrease in the percentage of depolarized cells (indicated by the decrease in relative fluorescence intensity of oxonol) in cells treated with kaempferol for 96 h, as compared with control (Fig. 3*C*). Addition of KCl depolarized the cells significantly, consistent with the generalized effect of KCl on $\Delta\psi_p$ (data not shown; ref. 24).

Increase in Membrane Fluidity of Glioblastoma Cells by Kaempferol

As ROS production affects plasma membrane fluidity (33) and because alterations in plasma membrane fluidity occur in cells exposed to various apoptotic stimuli (34), the membrane fluidity of control and kaempferol-treated glioma cells was determined using the fluorescent probe DPH. A significant 3- and 11-fold decrease in the membrane microviscosity of kaempferol-treated U87MG and LN229 cells, respectively, was observed as compared with control. Because microviscosity and fluidity are inversely correlated, these results indicated an increase in membrane fluidity of cells treated with kaempferol for 96 h (Fig. 3*C*).

Kaempferol Suppresses the Release of Proinflammatory Cytokines and Chemokines from Glioblastoma Cells

Because proinflammatory cytokines and chemokines can influence feed forward cycle of inflammation, redox balance, and migration associated with tumor progression, we carried out cytometric bead array to investigate the cytokine/chemokine profile of glioma cells treated with kaempferol for 96 h. A general trend toward decrease in the release of proinflammatory mediators was observed in kaempferol-treated gliomas. There was a significant 10- and 2-fold decrease in interleukin (IL)-6, ~8- and 2-fold decrease in IL-8, ~1.7- and 2-fold decrease in monocyte chemoattractant protein-1 (MCP-1), and ~2-fold ($P < 0.05$) decrease in regulated on activation, normal T-cell expressed and secreted (RANTES) expression in kaempferol-treated U87MG (Fig. 4*A*) and T98G (Fig. 4*B*) as compared with control.

To determine whether the ability of kaempferol to regulate cytokine/chemokine levels was ROS dependent,

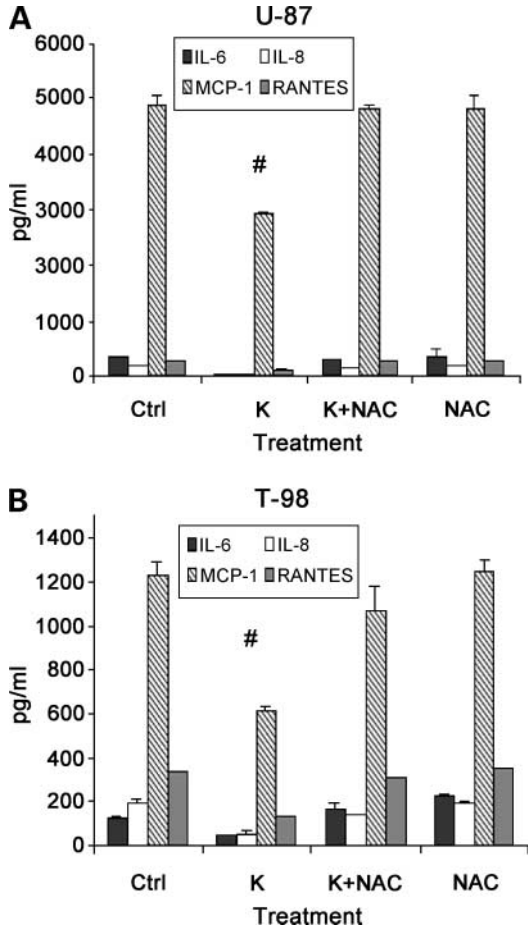

Figure 4. Kaempferol suppresses the release of proinflammatory cytokines and chemokines from glioblastoma. Expression of IL-6, IL-8, MCP-1, and RANTES in gliomas treated with kaempferol for 96 h in the presence or absence of NAC, as observed by cytometric bead array. Level of proinflammatory mediator was significantly suppressed in kaempferol-treated U87MG (**A**) and T98 (**B**) as compared with untreated control. Addition of NAC to kaempferol-treated cultures reversed the inhibitory effect of kaempferol significantly. **A** and **B,** *columns,* mean from three individual experiments; *bars,* SE. #, $P < 0.05$, significant decrease compared with control.

[1] Supplementary data for this article are available at Molecular Cancer Therapeutics Online (http://mct.aacrjournals.org/).

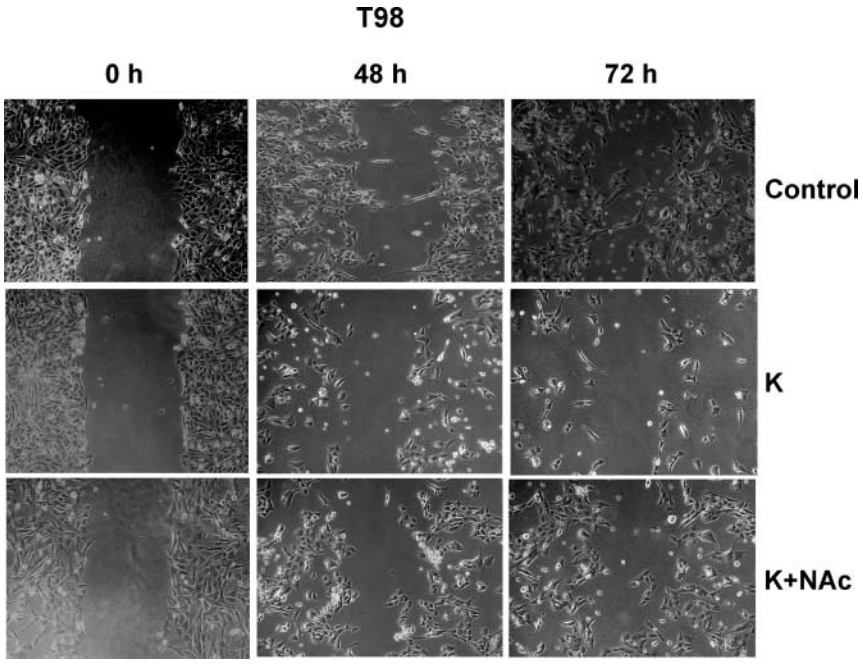

Figure 5. The ability of kaempferol to inhibit glioma cell migration is ROS dependent. The ability of T98G to migrate after scratch wound injury was inhibited in the presence of kaempferol, and this inhibition was reversed in the presence of ROS inhibitor NAC. Micrographs depict cultures of T98G with scratch wound, which were left untreated or treated with kaempferol for 48 and 72 h either in the presence or absence of NAC. Representative of two independent experiments with identical results.

the expression of these proinflammatory mediators was determined in cells treated with kaempferol in the presence of NAC. Treatment with NAC alone had no significant effect on the release of cytokines/chemokines from glioma cells. However, treatment with a combination of NAC and kaempferol reversed the inhibitory effect of kaempferol on proinflammatory cytokine/chemokine release because the level of proinflammatory mediators released from glioma treated with this combination was almost comparable to that of untreated control (Fig. 4*A* and *B*).

Kaempferol Inhibits Glioma Cell Migration in a ROS-Dependent Manner

Because both ROS and chemokines are crucial regulators of cancer cell migration and because ROS, IL-8, MCP-1, and RANTES levels were significantly altered in kaempferol-treated cells, we investigated the migration ability of gliomas in the absence and presence of kaempferol using wound healing assay. There was an obvious decrease in cell migration, as shown by the difference in the wound area covered in kaempferol-treated cells as compared with control. Although untreated cells migrated to cover the wound area as expected, treatment with kaempferol inhibited motility of T98G at different time points investigated (Fig. 5). The effects of kaempferol on wound healing were dependent on ROS because the ability of cells treated with a combination of NAC and kaempferol to migrate across the wound area was almost comparable to that of untreated control. A similar trend was observed in U87MG cells (data not shown).

Synergistic Induction of Apoptosis and Oxidative Stress in Human Glioma Cells by Kaempferol and Doxorubicin

Glioblastoma treatment is most often based on a combination of several drugs. Because doxorubicin, often used in chemotherapeutic regimen, induces apoptosis in glioblastoma (35), we evaluated whether kaempferol could enhance the cytotoxic effect of doxorubicin. Approximately 4- and 5-fold increase in apoptosis was observed in U87MG treated with kaempferol or doxorubicin, respectively, for 24 h, as compared with control. Interestingly, kaempferol potentiated the toxic effect of doxorubicin because a dramatic 18-fold increase in apoptotic cells was observed when U87MG cells were treated with doxorubicin in conjunction with kaempferol for 24 h (Fig. 6*A*).

To determine whether enhanced oxidative stress could have accounted for the synergistic interaction between kaempferol and doxorubicin, the level of ROS was determined in cells treated with doxorubicin or kaempferol, or a combination of both, for 24 h. Whereas a significant ~2.0- and 3.1-fold increase in ROS was observed in U87MG cells treated with kaempferol and doxorubicin, respectively, treatment with a combination of both further elevated ROS level by 4.5-fold as compared with control (Fig. 6*B*).

To determine whether kaempferol potentiated the cytotoxic effect of doxorubicin by enhancing its accumulation, we carried out FACS analysis to determine the ability of U87MG to efflux doxorubicin in treated cells relative to control. In comparison with control, which exhibited 40% doxorubicin efflux over a time course of 120 min following accumulation of doxorubicin, only 8% of doxorubicin was effluxed from cells treated with kaempferol for 96 h (Fig. 6*C*).

Discussion

The degree of oxidative stress in a cell reflects a balance between the rate of ROS production and the activity of

scavenging systems that detoxify them (5). Increased basal oxidative stress in transformed cells makes them highly dependent on their antioxidant systems to counteract the damaging effect of ROS (36) and this makes them susceptible to further oxidative insults (5, 36). Diverse chemotherapeutic agents can induce apoptosis in cancer cell lines through increased ROS generation (36, 37). Kaempferol is known to induce apoptosis in numerous cancer cell lines; however, its effect on glioma cells is not well understood. Our results show that kaempferol induces apoptosis in human glioma cells through increased ROS generation.

Increased ROS accumulation in kaempferol-treated gliomas was accompanied by a decrease in the levels of redox active proteins SOD-1 and TRX-1, which are involved in maintaining cellular redox balance. SOD-1 acts as a major defense against ROS by detoxifying the superoxide anion, and knockdown of SOD-1 expression induces cell death in malignant cells (38). Increased levels of TRX-1 in a variety of malignant tumors may contribute to the resistance of cancers to therapy by scavenging ROS, which are generated by various anticancer agents (39). Not only does down-regulation of SOD-1 expression increases sensitivity of tumor cells to the cytotoxic agents (28) but the anticancer activity of some flavonoids has also been attributed to their ability to inhibit thioredoxin reductase (10). Importantly, SOD and TRX have been implicated in the pathogenesis of astrocytomas (40). Our findings that siRNA-mediated down-regulation of SOD-1 and TRX-1 in gliomas increases ROS generation and enhances sensitivity to kaempferol-induced apoptosis are consistent with previous reports that inhibition of SOD (7) and TRX (29) enhances sensitivity of tumor cells to ROS-generating anticancer agents. Weakening of the antioxidant defense mechanism may contribute to the sensitivity of glioma to ROS because reduced levels of SOD-1 and TRX-1 might not be sufficient for handling, scavenging, and detoxifying the excessive ROS generated in kaempferol-treated glioma.

Kaempferol-mediated increase in ROS generation and decrease in $\Delta\Psi_m$ were concomitant with apoptosis, suggesting that severe accumulation of ROS in oncogenically transformed cells causes oxidative damage to mitochondrial membranes and impairs membrane integrity, leading to cell death (36, 37). Because membrane potential influences resistance of cancer cells to chemotherapeutics (24), it is possible that an altered $\Delta\psi_p$ plays a role in kaempferol-induced apoptosis. The fluidity of plasma membrane plays an important role in chemotherapy-induced cell death (41, 42) because changes in multidrug resistance are associated with alterations in the fluidity (43). An increase in membrane fluidity in kaempferol-treated cells could have increased the sensitivity of cells to doxorubicin, as previously reported (43). The inhibition of glioma cell migration by kaempferol in a ROS-dependent manner is consistent with previous reports of ROS involvement in tumor migration (44). ROS is known to down-regulate the expression of proinflammatory genes (45). Because MCP-1 increases aggressiveness of gliomas (46) and because both IL-6 (47) and IL-8 (48) contribute to proliferation and progression of glioblastoma, it is possible that kaempferol inhibits glioma cell migration by suppressing the release of proinflammatory cytokines/chemokines.

Because ROS toxicity induced by certain chemotherapeutic agents can be an effective means of eradicating malignant cells, it is useful to consider effective ways of achieving significant synergy through combination of agents with similar ability to alter redox conditions.

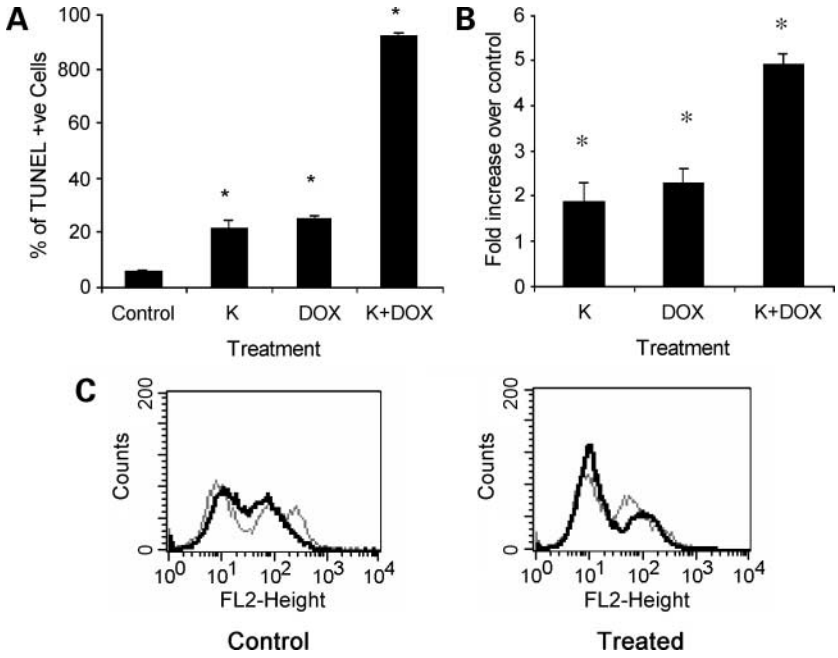

Figure 6. Kaempferol potentiates the toxic effect of doxorubicin. **A,** increase in the percentage of TUNEL-positive U87MG following treatment with a combination of kaempferol and doxorubicin. The graph represents the percentage of TUNEL-positive cells treated with kaempferol or doxorubicin, or a combination of both, for 24 h. **B,** treatment of U87MG with a combination of kaempferol and doxorubicin enhances the production of ROS dramatically as compared with untreated cells or cells treated with either kaempferol or doxorubicin. The graph indicates the level of ROS generated following treatment with doxorubicin or kaempferol, or a combination of both, for 24 h. **A** and **B,** *columns,* mean from three individual experiments; *bars,* SE. *, $P < 0.005$, significant increase compared with untreated control. **C,** differential doxorubicin accumulation and efflux in untreated and kaempferol-treated cells (96 h). Cells were incubated with doxorubicin for 30 min and subsequently washed, and intracellular doxorubicin content was measured by FACS at the FL2 spectrum immediately at $t = 0$ for accumulation and at $t = 120$ min to allow for efflux. *Left,* untreated; *right,* kaempferol treated. *Dark line,* $t = 120$; *dotted line,* $t = 0$. *DOX,* doxorubicin.

Doxorubicin, often included in chemotherapy regimens, has several mechanisms of action; one of which is the formation of free radicals leading to oxidative stress (49). Kaempferol potentiated the toxic effect of doxorubicin by amplifying ROS generation. The ability of kaempferol to enhance intracellular accumulation of doxorubicin by reducing its efflux agrees with previous studies that flavonoids reverse multidrug resistance involved in regulating the efflux of chemotherapeutic drugs from cells (50). It is possible that kaempferol exacerbated doxorubicin-induced damage in glioma cells by coupling enhanced oxidative stress with increased accumulation of doxorubicin. Increased efficacy of kaempferol in inducing apoptosis of human glioma cells through modulation of cellular redox balance, in conjunction with other ROS-generating anticancer therapeutic modalities, suggests that a strategy combining these agents warrants further investigation in glioblastoma.

Acknowledgments

We thank Uttam Kumar Saini for excellent technical assistance, Prof. Vijayalakshmi Ravindranath (Director, National Brain Research Centre) for her continuous support, and Dr. Anirban Basu (National Brain Research Centre) for his valuable suggestions.

References

1. Halliwell B. Reactive oxygen species and the central nervous system. J Neurochem 1992;59:1609 – 23.

2. Szatrowski TP, Nathan CF. Production of large amounts of hydrogen peroxide by human tumor cells. Cancer Res 1991;51:794 – 8.

3. Hu Y, Rosen DG, Zhou Y, et al. Mitochondrial manganese-superoxide dismutase expression in ovarian cancer: role in cell proliferation and response to oxidative stress. J Biol Chem 2005;280:39485 – 92.

4. Pelicano H, Feng L, Zhou Y, et al. Inhibition of mitochondrial respiration: a novel strategy to enhance drug-induced apoptosis in human leukemia cells by a reactive oxygen species-mediated mechanism. J Biol Chem 2003;278:37832 – 9.

5. Schumacker PT. Reactive oxygen species in cancer cells: live by the sword, die by the sword. Cancer Cell 2006;10:175 – 6.

6. Huang P, Feng L, Oldham EA, Keating MJ, Plunkett W. Superoxide dismutase as a target for the selective killing of cancer cells. Nature 2000; 407:390 – 5.

7. Zhou Y, Hileman EO, Plunkett W, Keating MJ, Huang P. Free radical stress in chronic lymphocytic leukemia cells and its role in cellular sensitivity to ROS-generating anticancer agents. Blood 2003;101: 4098 – 104.

8. Ross JA, Kasum CM. Dietary flavonoids: bioavailability, metabolic effects, and safety. Annu Rev Nutr 2002;22:19 – 34.

9. Wang IK, Lin-Shiau SY, Lin JK. Induction of apoptosis by apigenin and related flavonoids through cytochrome *c* release and activation of caspase-9 and caspase-3 in leukaemia HL-60 cells. Eur J Cancer 1999; 35:1517 – 25.

10. Lu J, Papp LV, Fang J, et al. Inhibition of Mammalian thioredoxin reductase by some flavonoids: implications for myricetin and quercetin anticancer activity. Cancer Res 2006;66:4410 – 8.

11. Nguyen TT, Tran E, Ong CK, et al. Kaempferol-induced growth inhibition and apoptosis in A549 lung cancer cells is mediated by activation of MEK-MAPK. J Cell Physiol 2003;197:110 – 21.

12. Dimas K, Demetzos C, Mitaku S, et al. Cytotoxic activity of kaempferol glycosides against human leukaemic cell lines *in vitro*. Pharmacol Res 2000;41:83 – 6.

13. Shen SC, Lin CW, Lee HM, Chien LL, Chen YC. Lipopolysaccharide plus 12-*O*-tetradecanoylphorbol 13-acetate induction of migration and invasion of glioma cells *in vitro* and *in vivo*: differential inhibitory effects of flavonoids. Neuroscience 2006;140:477 – 89.

14. Iida T, Furuta A, Kawashima M, et al. Accumulation of 8-oxo-2′-deoxyguanosine and increased expression of hMTH1 protein in brain tumors. Neuro-oncol 2001;3:73 – 81.

15. Silber JR, Bobola MS, Blank A, et al. The apurinic/apyrimidinic endonuclease activity of Ape1/Ref-1 contributes to human glioma cell resistance to alkylating agents and is elevated by oxidative stress. Clin Cancer Res 2002;8:3008 – 18.

16. Bestwick CS, Milne L, Pirie L, Duthie SJ. The effect of short-term kaempferol exposure on reactive oxygen levels and integrity of human (HL-60) leukaemic cells. Biochim Biophys Acta 2005;1740: 340 – 9.

17. Lee ER, Kang YJ, Kim JH, Lee HT, Cho SG. Modulation of apoptosis in HaCaT keratinocytes via differential regulation of ERK signaling pathway by flavonoids. J Biol Chem 2005;280:31498 – 507.

18. Ravid A, Rocker D, Machlenkin A, et al. 1,25-Dihydroxyvitamin D3 enhances the susceptibility of breast cancer cells to doxorubicin-induced oxidative damage. Cancer Res 1999;59:862 – 7.

19. Rahmani M, Reese E, Dai Y, et al. Coadministration of histone deacetylase inhibitors and perifosine synergistically induces apoptosis in human leukemia cells through Akt and ERK1/2 inactivation and the generation of ceramide and reactive oxygen species. Cancer Res 2005;65: 2422 – 32.

20. Mukherjee SB, Das M, Sudhandiran G, Shaha C. Increase in cytosolic Ca^{2+} levels through the activation of non-selective cation channels induced by oxidative stress causes mitochondrial depolarization leading to apoptosis-like death in *Leishmania donovani* promastigotes. J Biol Chem 2002;277:24717 – 27.

21. Gitlin L, Karelsky S, Andino R. Short interfering RNA confers intracellular antiviral immunity in human cells. Nature 2002;418:430 – 4.

22. Sen E, Bromberg-White JL, Meyers C. Genetic analysis of cis regulatory elements within the 5′ region of the human papillomavirus type 31 upstream regulatory region during different stages of the viral life cycle. J Virol 2002;76:4798 – 809.

23. Basu A, Krady JK, O'Malley M, et al. The type 1 interleukin-1 receptor is essential for the efficient activation of microglia and the induction of multiple proinflammatory mediators in response to brain injury. J Neurosci 2002;22:6071 – 82.

24. Liang XJ, Yin JJ, Zhou JW, et al. Changes in biophysical parameters of plasma membranes influence cisplatin resistance of sensitive and resistant epidermal carcinoma cells. Exp Cell Res 2004; 293:283 – 91.

25. Frank NY, Margaryan A, Huang Y, et al. ABCB5-mediated doxorubicin transport and chemoresistance in human malignant melanoma. Cancer Res 2005;65:4320 – 33.

26. Sen E, Chattopadhyay S, Bandopadhyay S, De T, Roy S. Macrophage heterogeneity, antigen presentation, and membrane fluidity: implications in visceral leishmaniasis. Scand J Immunol 2001;53:111 – 20.

27. Soldan SS, Alvarez Retuerto AI, Sicotte NL, Voskuhl RR. Dysregulation of IL-10 and IL-12p40 in secondary progressive multiple sclerosis. J Neuroimmunol 2004;146:209 – 15.

28. Ding WQ, Vaught JL, Yamauchi H, Lind SE. Differential sensitivity of cancer cells to docosahexaenoic acid-induced cytotoxicity: the potential importance of down-regulation of superoxide dismutase 1 expression. Mol Cancer Ther 2004;3:1109 – 17.

29. Ungerstedt JS, Sowa Y, Xu WS, et al. Role of thioredoxin in the response of normal and transformed cells to histone deacetylase inhibitors. Proc Natl Acad Sci U S A 2005;102:673 – 8.

30. Campian JL, Qian M, Gao X, Eaton JW. Oxygen tolerance and coupling of mitochondrial electron transport. J Biol Chem 2004;279:46580 – 7.

31. Klyubin IV, Kirpichnikova KM, Ischenko AM, Zhakhov AV, Gamaley IA. The role of reactive oxygen species in membrane potential changes in macrophages and astrocytes. Membr Cell Biol 2000;13:557 – 66.

32. Samhan-Arias AK, Martin-Romero FJ, Gutierrez-Merino C. Kaempferol blocks oxidative stress in cerebellar granule cells and reveals a key role for reactive oxygen species production at the plasma membrane in the commitment to apoptosis. Free Radic Biol Med 2004;37:48 – 61.

33. Sergent O, Pereira M, Belhomme C, et al. Role for membrane fluidity in ethanol-induced oxidative stress of primary rat hepatocytes. J Pharmacol Exp Ther 2005;313:104 – 11.

34. Fujimoto K, Iwasaki C, Kawaguchi H, Yasugi E, Oshima M. Cell membrane dynamics and the induction of apoptosis by lipid compounds. FEBS Lett 1999;446:113 – 6.

35. Stan AC, Casares S, Radu D, Walter GF, Brumeanu TD. Doxorubicin-induced cell death in highly invasive human gliomas. Anticancer Res 1999; 19:941 – 50.

36. Trachootham D, Zhou Y, Zhang H, et al. Selective killing of oncogenically transformed cells through a ROS-mediated mechanism by β-phenylethyl isothiocyanate. Cancer Cell 2006;10:241 – 52.

37. Yu R, Mandlekar S, Harvey KJ, Ucker DS, Kong AN. Chemopreventive isothiocyanates induce apoptosis and caspase-3-like protease activity. Cancer Res 1998;58:402 – 8.

38. Blander G, de Oliveira RM, Conboy CM, Haigis M, Guarente L. Superoxide dismutase 1 knock-down induces senescence in human fibroblasts. J Biol Chem 2003;278:38966 – 9.

39. Marks PA. Thioredoxin in cancer-role of histone deacetylase inhibitors. Semin Cancer Biol 2006;16:436 – 43.

40. Haapasalo H, Kylaniemi M, Paunul N, Kinnula VL, Soini Y. Expression of antioxidant enzymes in astrocytic brain tumors. Brain Pathol 2003;13:155 – 64.

41. Dimanche-Boitrel MT, Meurette O, Rebillard A, Lacour S. Role of early plasma membrane events in chemotherapy-induced cell death. Drug Resist Updat 2005;8:5 – 14.

42. Lacour S, Hammann A, Grazide S, et al. Cisplatin-induced CD95 redistribution into membrane lipid rafts of HT29 human colon cancer cells. Cancer Res 2004;64:3593 – 8.

43. Schuldes H, Dolderer JH, Zimmer G, et al. Reversal of multidrug resistance and increase in plasma membrane fluidity in CHO cells with R-verapamil and bile salts. Eur J Cancer 2001;37:660 – 7.

44. Wu WS. The signaling mechanism of ROS in tumor progression. Cancer Metastasis Rev 2006;25:695 – 705.

45. Mathy-Hartert M, Martin G, Devel P, et al. Reactive oxygen species down-regulate the expression of pro-inflammatory genes by human chondrocytes. Inflamm Res 2003;52:111 – 8.

46. Platten M, Kretz A, Naumann U, et al. Monocyte chemoattractant protein-1 increases microglial infiltration and aggressiveness of gliomas. Ann Neurol 2003;54:388 – 92.

47. Weissenberger J, Loeffler S, Kappeler A, et al. IL-6 is required for glioma development in a mouse model. Oncogene 2004;23: 3308 – 16.

48. Wakabayashi K, Kambe F, Cao X, et al. Inhibitory effects of cyclosporin A on calcium mobilization-dependent interleukin-8 expression and invasive potential of human glioblastoma U251MG cells. Oncogene 2004;23:6924 – 32.

49. Gewirtz DA. A critical evaluation of the mechanisms of action proposed for the antitumor effects of the anthracycline antibiotics Adriamycin and daunorubicin. Biochem Pharmacol 1999;57:727 – 41.

50. Imai Y, Tsukahara S, Asada S, Sugimoto Y. Phytoestrogens/flavonoids reverse breast cancer resistance protein/ABCG2-mediated multidrug resistance. Cancer Res 2004;64:4346 – 52.